nature portfolio

https://doi.org/10.1038/s41565-022-01126-z

Supplementary information

Atomic-scale friction between single-asperity contacts unveiled through in situ transmission electron microscopy

In the format provided by the authors and unedited

Supplementary Information

for

Atomic-scale friction between single-asperity contacts unveiled through in-situ Transmission Electron Microscopy

Wang et al.

This supplementary information file includes:

1. **Supplementary Figures 1-6**
2. **Supplementary Discussion 1-3**
3. **Supplementary Tables 1-2**
4. **Supplementary References**

Supplementary Figures

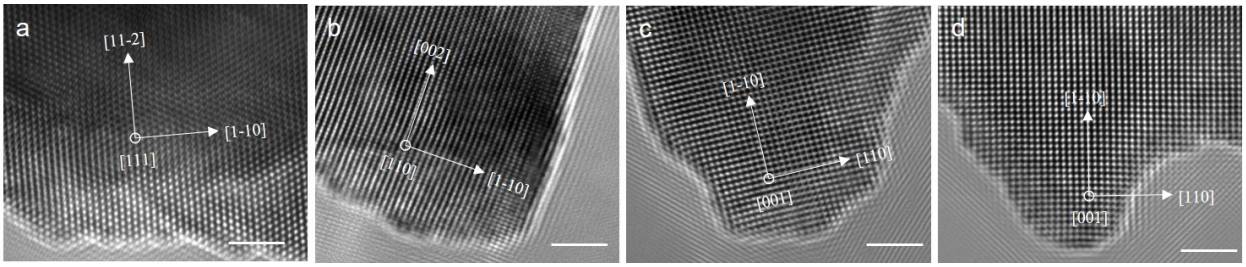

Supplementary Figure 1. Tungsten substrates with different orientations. (a) [111] orientation. (b) [110] orientation. (c) [001] orientation. (d) [001] orientation with horizontal (1-10) surface. Scale bar 2 nm.

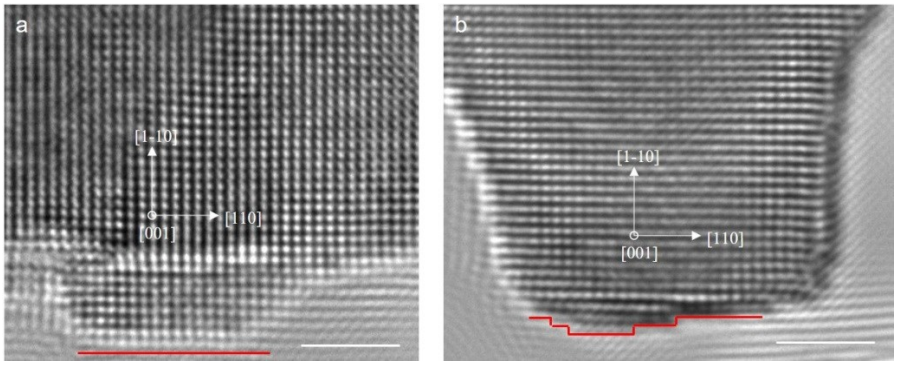

Supplementary Figure 2. The substrates with smooth and defective surfaces. (a) The smooth (1-10) surface. (b) The defected (1-10) surface with steps. Scale bar 2 nm.

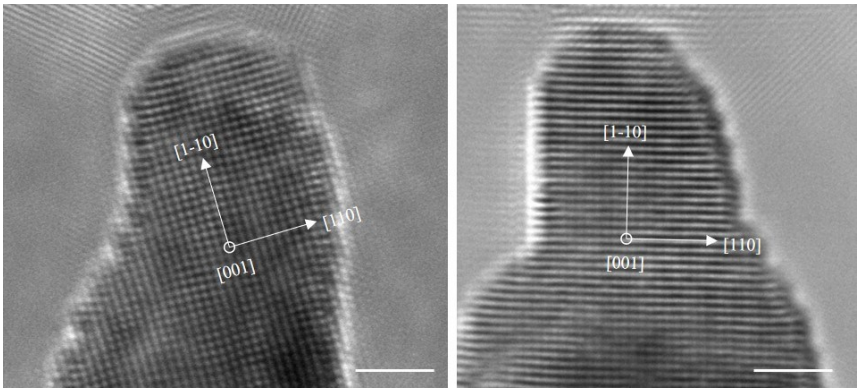

Supplementary Figure 3. The prepared tip asperity. Scale bar 2 nm.

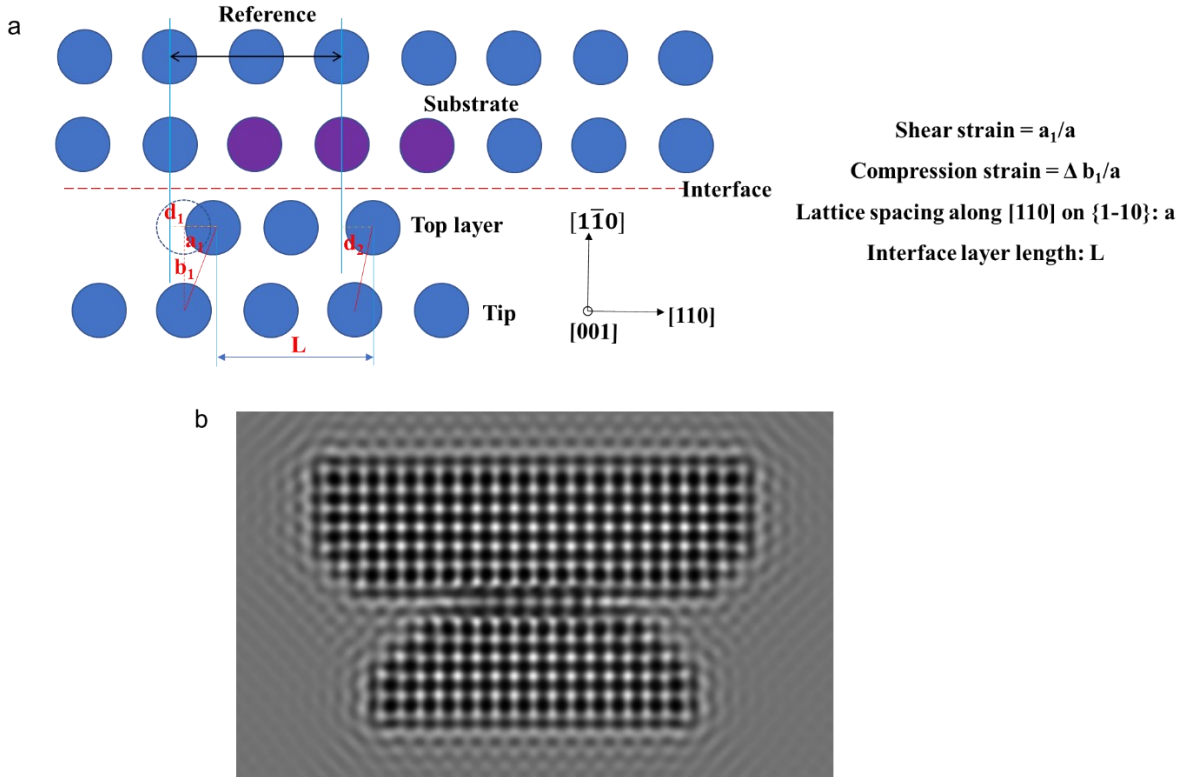

Supplementary Figure 4. The lattice measurement in frciton. (a)Schematic of lattice strain measurement. *a* is the interplane distance between {110} planes, a_1 is the deviation distance between atoms on the top layer and the neighboring layer along [110] (horizontal direction), b_1 is

the distance between atoms on the top layer and the neighboring layer along [1-10] (vertical direction), d_1 and d_2 are the displacements of the leftmost and rightmost atoms in the top layer relative to the reference layer in the substrate. L is the length of the top layer. The layer is assumed to be in a square shape and the layer area to be L^2. The shear strain can be calculated as a_1/a and the compression strain can be calculated as $\Delta b_1/a$. The shear force can be estimated as $\overline{a_1/a}$ • *G (shear modulus)* • L^2 and the compression force can be estimated as $\overline{\Delta b_1/a}$ • *E (Young's modulus)* • L^2. Seven atoms on the top layer of the tip were selected to calculate the average strain in the experiment. Notably, due to the vibration of the shear strain at different sites, the calculated shear force is suspected to possess a large error bar. (b) Simulated high-resolution TEM image of the atomic friction between two W asperities. The simulation parameter: the accelerating voltage: 200 keV, the spherical aberration: 0.2 mm, defocus: −4 nm, thickness: 24 nm. The bright features in the simulated image represent the atom columns and the center of the bright atom column could be regarded as the position of the atom, implying that using the intensity profile of the atom columns to determine the lattice strain is acceptable.

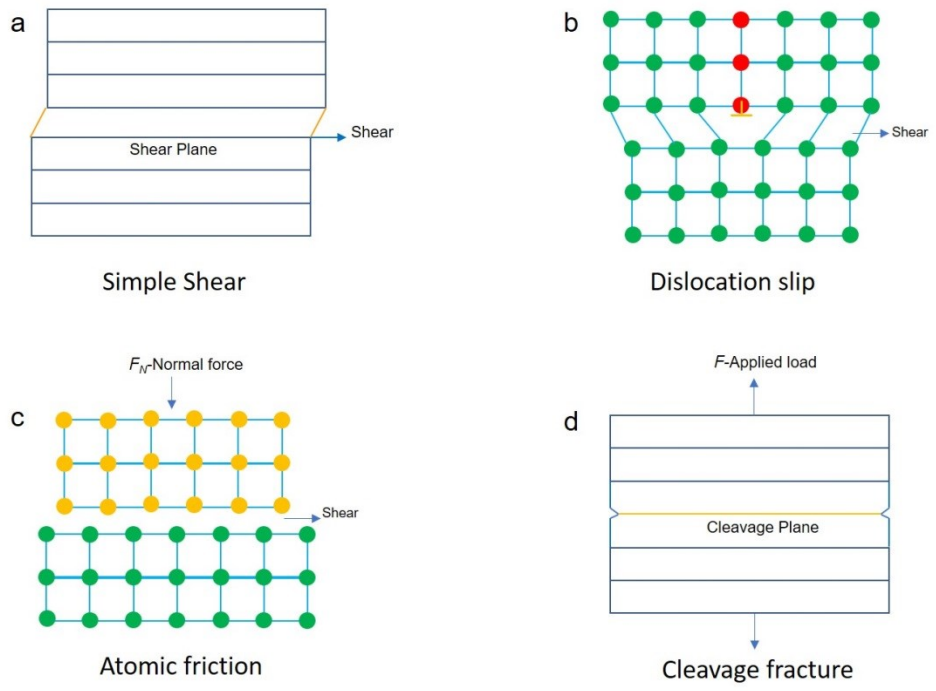

Supplementary Figure 5. The material strengths defined under different models. (a) The simple shear. (b) The dislocation slip under the shear. (c) The friction. (d) The cleavage fracture under tension.

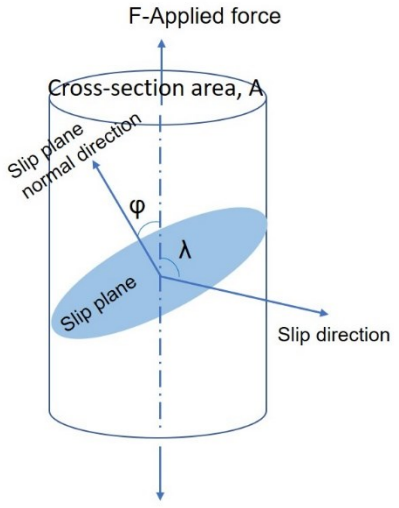

$$\tau_{rss} = \frac{F \cdot cos\lambda}{A/cos\varphi} = \sigma \cdot cos\varphi cos\lambda = \sigma \cdot m$$

$$\gamma = \frac{Fcos\lambda}{Fcos\varphi} = cos\lambda/cos\varphi$$

Supplementary Figure 6. The uniaxial loading of a single crystal.

Supplementary Table 1. The relative displacement of interface atoms from points 2 to 3 in Fig. 2a. (unit: Å)

Interface atom number/Direction	x [110]	y[1$\bar{1}$0]	z[001]
1	0.026198	-0.18915	0.005271
2	-0.13268	-0.00142	-0.06139
3	-0.32188	-0.01711	-0.13805
4	-0.29757	-0.00079	-0.12531
5	-0.32478	0.059199	-0.17242
6	-0.00378	-0.03521	-0.06379
7	0.148885	-0.19921	0.060586
8	0.027819	-0.1188	0.067993
9	-0.34402	0.033322	0.159406
10	-0.11053	-0.00513	0.046841
11	0.062593	-0.03934	0.112298
12	-0.15267	-0.02608	0.242679
13	-0.36239	0.034183	0.025089
14	0.098244	-0.16744	-0.02769
15	0.239432	-0.06228	0.062054
16	0.385684	-0.14315	0.03383
17	0.21114	0.043547	0.017282
18	0.124375	0.030212	0.073398
19	0.268399	-0.05976	0.016414
20	-0.47434	0.087425	-0.03556
21	-0.59014	0.062905	-0.02142
22	0.436258	-0.22922	0.120706
23	0.072788	-0.11714	-0.0816
24	-0.56556	0.010324	-0.06012
25	0.228899	0.010556	0.010409
26	0.32775	-0.03352	0.178423
27	-0.22275	0.04818	0.033162
28	0.095206	0.017207	-0.08621
29	0.168062	0.06082	0.014079
30	0.312963	-0.07637	-0.1492
31	0.274071	-0.07263	-0.01782
Average	~-0.013	~-0.035	~0.01

Supplementary Discussion

1. Elastic modulus calculation

The Young's modulus E_{ijk} of body-centered cubic (BCC) crystals along [ijk] direction could be calculated by the equation[1]:

$$E_{ijk} = \left\{S_{11} - 2\left(S_{11} - S_{12} - \frac{S_{44}}{2}\right) \cdot \left(l_{i1}^2 l_{j2}^2 + l_{k3}^2 l_{j2}^2 + l_{i1}^2 l_{k3}^2\right)\right\}^{-1} \quad (1)$$

where S_{11}, S_{12}, S_{44} are the elastic compliances; l_{i1}, l_{j2}, l_{k3} are the direction cosines. The shear modulus of {110} in cubic crystals along <11$\bar{1}$> and <1$\bar{1}$0> could be calculated by the equations respectively[2]:

$$G_{\{110\}<11\bar{1}>} = \left(\frac{3}{1+2A}\right) C_{44} \quad (2)$$

$$G_{\{110\}<1\bar{1}0>} = {C_{44}}/{A} \quad (3)$$

Where C_{44} is the elastic constant and A is the anisotropy factor. For tungsten single crystal at ambient temperature, the elastic constant and compliances are C_{44} = 151.4 GPa, S_{11} = 0.257×10^{-2} GPa^{-1}, S_{12} = -0.073×10^{-2} GPa^{-1}, S_{44} = 0.66×10^{-2} GPa^{-1}, and A is 1.01 respectively[3]. Based on the above equations, Young's modulus and shear modulus for W single crystal can be obtained as follows: $E_{100} = E_{110}$ = 389 GPa, $G_{\{110\}<1\bar{1}0>}$ = 150 GPa, $G_{\{110\}<11\bar{1}>}$ = 150.4 GPa.

2. The estimation of the friction coefficiency

In the experiment, the average friction force $\overline{F_f} = \frac{\int_0^x F_f dx}{x} \approx 16.26$ nN (Fig. 1a) and the average normal force $\overline{F_n} = \frac{\int_0^x F_n dx}{x} \approx 41.36$ nN (Extended Data Fig. 3). The friction coefficient can be estimated as $\mu_{ex} = \frac{\overline{F_f}}{\overline{F_n}} \approx 0.39$. For the case with 11 contact atoms, as shown in Fig. 3 and

Extended Data Fig.7, the average friction force and normal force are 32.16 nN and 126.63 nN respectively. And its corresponding friction coefficient is ~0.25. In MD simulation, the average friction force $\overline{F_f} = \frac{\int_0^x F_f dx}{x} \approx 6.53$ nN (Fig. 2a) and the average normal force $\overline{F_n} = \frac{\int_0^x F_n dx}{x} \approx 30.51$ nN (Extended Data Fig. 1). Thus the friction coefficient can be estimated as $\mu_{MD} = \frac{\overline{F_f}}{\overline{F_n}} \approx 0.21$. For the case with 11 contact atoms in MD simulation, the estimated friction coefficient is ~0.43.

3. The material strengths defined under different loading conditions

Based on the second law of thermodynamics, one criterion was proposed to evaluate the crystal stability under deformation that the change of Helmholtz free energy is larger than or equal to the mechanical work done by the applied stress $\delta F \geq \delta W$.[4] According to this criterion, the ideal strength of BCC metals could be estimated as $0.11G$ under simple shear, (Supplementary Fig. 5a) and the cleavage fracture strength is about $0.083E$ under uniaxial tension (Supplementary Fig. 5d).[5] Generally, the shear occurs on {110} planes along <111> direction and the weakest fracture plane is {100} in BCC metals.[5] The ideal cleavage strength indicates the bonding strength between atoms within the crystal. It is generally recognized that the kink-pair mechanism governs the movement of screw dislocations in BCC metals.[6] The behaviors of edge dislocations are akin to ones in Face-centered cubic (FCC) metals.[7] The single-asperity friction was designed here to perform on {110} plane, which is a common slip plane in BCC metals,[5] between two separate tungsten crystals with the same orientation. Similarly, the resistance encountered in the slipping within a BCC crystal gives the criteria to evaluate the materials' strength. The strengths such as the yield strength can be assessed through measuring critical stresses for the motion of dislocations leading to the permanent plastic deformation (Supplementary Fig. 5c and Supplementary Fig. 6). Either the simple shear or the dislocation slipping requires to overcome the lattice friction.

Nonetheless, the dislocation-mediated slipping can be regarded as a fractional counter-motion between two parts of the crystal rather than the overall rigid movement in the friction process or under simple shear. If misfit dislocation-mediated the shearing in the interface layer, the movement of interlayer atoms should follow the slipping trace of 1/2[111] dislocation along [111] on $(1\bar{1}0)$ plane. Considering the stress state influences the critical stress for dislocation slip, the applied compression force in contact should increase the threshold value for activating the dislocation nucleation in friction.[8] The maximum resolve shear stress could provide the driving force for dislocation nucleation, but the dislocation-assisted slipping in the friction process is expected to exist in a large contact region where the dislocation could nucleate and pile up stably.[9, 10] The range of contact radius for the single-dislocation-assisted slip in friction is normally within 10 nm-10 μm.[9] When the contact area is lower than the critical value, the friction force is supposed to be at the same order of magnitude with the ideal shear strength,[9, 11] consistent with our experimental results (the contact area is only 1.54-5.24 nm^2). Strengths of tungsten defined under various loading conditions were collected in Supplementary Table 2. It is found that the maximum shear stress encountered (~12.9 and ~10.1 GPa for cases with 7 and 11 contact atoms respectively in the experiment and ~16.4 and ~ 18.2 GPa for two cases respectively in MD) in friction studied here was close to the ideal strength (~16.5 GPa), much higher than the values for dislocation slip (~2.5 GPa for screw and ~0.06 GPa for edge), which exemplified that the local fractional shear mediated by the defect motion is much easy in real crystals[5]. This also suggested that the discrete stick-slip may not be easily explained by the dislocation-assisted slip model[9, 12]. For a single crystal under uniaxial loading, as shown in Supplementary Fig. 6, the resolved shear stress τ_{rss} can be calculated by $\tau_{rss} = \frac{F \cdot cos\lambda}{A/cos\varphi} = \sigma \cdot cos\varphi cos\lambda = \sigma \cdot m$, where σ is the applied stress, F is the loading force, A is the cross-section area, and φ, λ are the angles between the loading direction and

the normal direction of the slip plane, the slip direction respectively. Coefficient *m* is called the Schmid factor.[13] The ratio between the normal force with the resolved shear force γ can be expressed as $\gamma = \frac{F\cos\lambda}{F\cos\varphi} = {\cos\lambda}/{\cos\varphi}$. The critical resolved shear stress τ_{crss} activating the motion of dislocations is normally definite in one material. But for BCC metals, there exist multiple slipping systems and the dislocation slipping normally occurs on {110} plane along <111> direction at ambient condition.[14] The critical resolved shear stress τ_{crss} is associated with the loading condition and the local stress state, which deviates from the traditional Schmid Law.[15]

Supplementary Table 2. The strengths defined under different conditions for W single crystal.

Definition	Loading condition	Reference Value (GPa)	
Ideal strength	Simple shear[5]	{110}<1$\bar{1}$0> 16.54	{110}<111> 16.5
Critical stress for the dislocation slip	Uniaxial loading	Edge[6] 0.056-0.075	Screw[15] ~2.5
Maximum shear stress Experiment	Friction under compression The case with 7 contact atoms	{110}<1$\bar{1}$0> ~18.9	{110}<111> ~12.9
	The case with 11 contact atoms	~14.7	~10.1
Maximum shear stress MD simulation	Friction under compression The case with 7 contact atoms	{110}<1$\bar{1}$0> ~20.1	{110}<111> ~16.4
	The case with 11 contact atoms	~22.3	~18.2

Supplementary References

1. Ting TCT. On Anisotropic Elastic Materials for which Young's Modulus E(n) is Independent of n or the Shear Modulus G(n,m) is Independent of n and m. *Journal of Elasticity* 2006, **81**(3)**:** 271-292.

2. Knowles KM, Howie PR. The Directional Dependence of Elastic Stiffness and Compliance Shear Coefficients and Shear Moduli in Cubic Materials. *Journal of Elasticity* 2015, **120**(1)**:** 87-108.

3. Meyers MA, Chawla KK. *Mechanical behavior of materials*. Cambridge university press, 2008.

4. Hill R, Milstein F. Principles of stability analysis of ideal crystals. *Physical Review B* 1977, **15**(6)**:** 3087.

5. Krenn C, Roundy D, Morris Jr J, Cohen ML. Ideal strengths of bcc metals. *Materials Science and Engineering: A* 2001, **319:** 111-114.

6. Liu X, Golubov SI, Woo CH, Huang H. Glide of edge dislocations in tungsten and molybdenum. 2004, **365**(1-2)**:** 96-100.

7. Tang M, Kubin L, Canova G. Dislocation mobility and the mechanical response of bcc single crystals: a mesoscopic approach. *Acta Materialia* 1998, **46**(9)**:** 3221-3235.

8. So M, Jacobsen KW, Stoltze P. Simulations of atomic-scale sliding friction. *Physical Review B* 1996, **53**(4)**:** 2101.

9. Hurtado JA, Kim KS. Scale effects in friction of single–asperity contacts. I. From concurrent slip to single–dislocation–assisted slip. *Proceedings of the Royal Society of London Series A: Mathematical, Physical and Engineering Sciences* 1999, **455**(1989)**:** 3363-3384.

10. Hurtado JA, Kim KS. Scale effects in friction of single–asperity contacts. II. Multiple–dislocation–cooperated slip. *Proceedings of the Royal Society of London Series A: Mathematical, Physical and Engineering Sciences* 1999, **455**(1989)**:** 3385-3400.

11. Carpick R, Agrait N, Ogletree D, Salmeron M. Variation of the interfacial shear strength and adhesion of a nanometer-sized contact. *Langmuir* 1996, **12**(13)**:** 3334-3340.

12. Dong Y, Li Q, Wu J, Martini A. Friction, slip and structural inhomogeneity of the buried interface. *Modelling and Simulation in Materials Science and Engineering* 2011, **19**(6)**:** 065003.

13. Schmid E, Boas W. *Kristallplasticität mit besonderer Berücksichtigung der Metalle*. JW Edwards, 1935.

14. Chin GJMT. Competition among {110},{112}, and {123}< 111> slip modes in BCC metals. 1972, **3**(8)**:** 2213-2216.

15. Srivastava K, Gröger R, Weygand D, Gumbsch P. Dislocation motion in tungsten: atomistic input to discrete dislocation simulations. *International Journal of Plasticity* 2013, **47:** 126-142.